A Moment-method Analysis of a Thin-wire Chireix-coil Antenna

A. A. Ayorinde[1], **S. A. Adekola**[1, 2], **and A. Ike Mowete**[1]

[1]Department of Electrical and Electronics Engineering
Faculty of Engineering, University of Lagos, Nigeria
[2]Department of Electrical and Electronics Engineering
Niger Delta University, Wilberforce Island, Yenegoa, Nigeria

Abstract— Using a moment-method solution technique in an Electric-Field Integral Equation (EFIE) formulation approach, this presentation examines certain performance characteristics of the electrically thin-wire variety of the Chireix-coil antenna, whose geometry as defined by [2] is given by $C_\lambda = \sqrt{1 + 2S_\lambda}$, where the parameters ($C_\lambda$, S_λ), respectively symbolize helix circumference and turn spacing, measured in units of wavelength at the operating frequency.

Computational results obtained for the Chireix coil with 4-, 6-, 8-, and 10-turns suggest that the maximum value of magnitude of current distributed along the axis of the antenna is more or less independent of number of antenna turns. And the results also indicate that when S_λ is less than 0.9, the radiation field (E_θ, E_φ) patterns on the azimuthal plane consist of two diametrically directed majors; which degenerate into four distinct lobes (with relative maxima along $\varphi = 0°$, 90°, 180°, and 270° axes) for values of S_λ in excess of 1.0. A particularly remarkable feature of these radiation field pattern characteristics is that they appear to be independent of the number of coil turns.

1. INTRODUCTION

When, for the thin-wire circular helical antenna, size of circumference (denoted by (C_λ) and measured in units of wavelength) lies between 0.75 and 1.3, the antenna radiates maximally in its axial direction, and is consequently commonly referred to as the axial-mode helix [2]. On the other hand, for values of C_λ less than 0.75, the helix antenna directs its radiation principally in the plane perpendicular to the helix axis, which is why it is designated as the normal-mode helix [4]. Although these two modes represent the principal radiation modes of the helical antenna, a few other important radiation modes such as octafilar-axial, quadrifilar-axial, backfire, and four-lobed (Chireix coil) have been developed and put to practical applications [2]. The focus of this presentation is on the Chireix coil (four-lobed mode), which as far as we can ascertain, has received little analytical attention in the open literature, and whose geometry, according to [2], is defined by $C_\lambda = \sqrt{1 + 2S_\lambda}$, making the simple realization of helical antennas with dimension C_λ greater than 1.3, a possibility.

The Chireix coil is modeled as an electrically thin structure and the approximate distribution of current along its axis is determined through a moment-method solution of the Electric Field Integral Equation (EFIE) formulated for the antenna problem. This current profile is then introduced in the radiation field integrals for the antenna, to determine the radiation field patterns, with emphasis solely on the azimuthal plane patterns following [5], who treated the case of a centre-fed microstrip helical antenna. Computational results generated for 4-, 6-, 8-, and 10-turn Chireix coils operating at the frequency of 3 GHz, and the Chireix coils physical parameters in the ranges $1.10 \leq C_\lambda \leq 2.15$ and $0.10 \leq S_\lambda \leq 1.80$ are displayed in graphical formats. A particularly interesting observation arising from these results is that they clearly suggest that the Chireix coil antenna's current profiles and associated azimuthal-plane radiation patterns are somewhat independent of the number of coil turns.

2. ELECTRIC-FIELD INTEGRAL EQUATION (EFIE) FORMULATION

Figure 1(a) depicts a Chireix-coil antenna which is essentially a thin-wire helix of circular cross-section excited at its geometrical centre, in which the position vector $\bar{r}'$ from the coordinate system origin to any point on the helical wire axis is expressible as:

$$\bar{r}' = a\cos\varphi'\hat{a}_x + a\sin\varphi'\hat{a}_y + (a\tan\alpha)\varphi'\hat{a}_z \tag{1}$$

where a represents the radius of the circular helix, α the helix pitch angle, and φ' the running variable along the helical wire axis. Figure 1(b) shows a complete turn of the coil of total length L_λ.

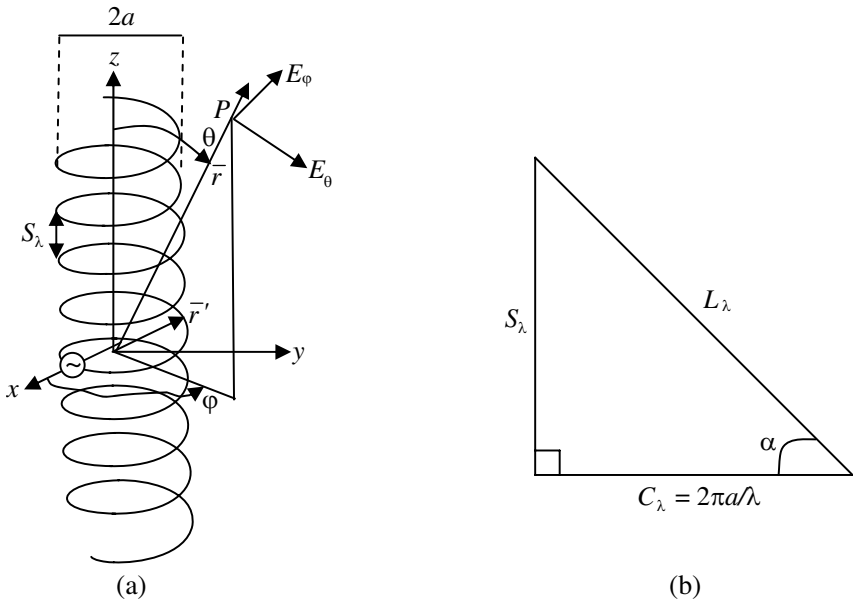

Figure 1: (a) A Chireix coil antenna excited at its geometrical centre; (b) a complete turn of the coil.

If it is assumed that the helical wire is perfectly conducting, then the total electric field on the helical wire surface, that is, the sum of incident electric field $\bar{E}^i$ and scattered electric field $\bar{E}^s$, satisfies the following boundary condition:

$$\hat{a}_n \times \left(\bar{E}^i + \bar{E}^s\right) = \bar{0} \tag{2}$$

in which $\hat{a}_n$ stands for the unit vector normal to the wire surface. Because the scattered electric field depends on the retarded scalar and vector potentials which can be expressed in terms of the induced current $I(\varphi')$, and upon the restriction of $I(\varphi')$ to the helical wire axis, it can be shown that the Electric Field Integral Equation (EFIE) governing the Chireix coil antenna problem posed here admits the form:

$$E^i_\varphi = L\ \left[I(\varphi')\right] \tag{3}$$

where

$$L[*] = \int_{-\pi N}^{\pi N} \left\{ \left[\cos\alpha\cos(\varphi-\varphi') + \tan\alpha\sin\alpha\right] \left[\frac{j\omega\mu_o a}{4\pi}\right][*] - \frac{1}{j4\pi\omega\varepsilon_o a\sec\alpha}\frac{d[*]}{d\varphi'}\frac{d}{d\varphi}\right\}\frac{e^{-jk_oR}}{R}d\varphi', \tag{4a}$$

and

$$R = a\sqrt{\left(\frac{r_w}{a}\right)^2 + 4\sin^2\left(\frac{\varphi-\varphi'}{2}\right) + \tan^2\alpha(\varphi-\varphi')^2} \tag{4b}$$

provided that the observation point φ is specified on the helical wire surface, r_w denotes the wire radius and N the number of coil turns. It should be remarked that the limits of the line integral $[-\pi N, \pi N]$ are the consequence of the fact that the helical antenna is excited at its geometrical centre which corresponds to the coordinate system origin. Of course the only unknown quantity in the EFIE above is $I(\varphi')$, the determination of which is effected via the moment-method technique in what follows.

3. MOMENT-METHOD SOLUTION OF THE EFIE

Towards the numerical solution of $I(\varphi')$ in the EFIE formulated above using the method of moments, we segment the helical structure into short lengths, and model the unknown quantity $I(\varphi')$ by the series representation:

$$I(\varphi') = \sum_{k=1}^{K} I_k T_k(\varphi') \tag{5}$$

where $T_k(\varphi')$ stands for triangular expansion functions of unit height, each defined over four consecutive segments, and I_k the unknown superposition coefficients. The substitution of Equation (5) in Equation (3) and taking the inner product of the resulting equation with the weighting functions $W_j(\varphi)$ defined over the helical surface and in the same manner as the expansion functions, we ultimately transform the EFIE into a matrix equation:

$$[V_j] = [Z_{jk}]\,[I_k] \tag{6}$$

in which $[Z_{jk}]$ is the generalized impedance matrix of the helical structure, $[V_j]$ the generalized voltage matrix which, in this case, has only one non-zero entry at the middle, and $[I_k]$ the generalized current matrix whose entries are the unknown superposition coefficients. The matrix inversion of $[Z_{jk}]$ and subsequent multiplication by the voltage matrix $[V_j]$ give the solution of $[I_k]$, that is,

$$I(\varphi'_k) = \sum_{k=1}^{K} [T_k(\varphi'_k)]\,[Z_{jk}]^{-1}\,[V_j] \tag{7}$$

which readily facilitates the computation of the electric fields radiated by the Chireix coil antenna. Using the vector potential approach, the radiated electric fields by the Chireix coil antenna are given by

$$E_\theta\,(\theta,\varphi) \;=\; \frac{-j\omega\mu_o a e^{-jk_o r}}{4\pi r} \int\limits_{-\pi N}^{\pi N} I(\varphi')[\cos\theta\sin(\varphi-\varphi') - \sin\theta\tan\alpha]e^{jk_o a\zeta\sin\theta}d\varphi', \tag{8a}$$

$$E_\varphi\,(\theta,\varphi) \;=\; \frac{-j\omega\mu_o a e^{-jk_o r}}{4\pi r} \int\limits_{-\pi N}^{\pi N} I(\varphi')[\cos(\varphi-\varphi')]e^{jk_o a\zeta\sin\theta}d\varphi', \tag{8b}$$

where

$$\zeta = \cos(\varphi-\varphi') + (\tan\alpha\cot\theta)\varphi'. \tag{8c}$$

For the numerical evaluation of the electric field components, we replace $I(\varphi')$ by Equation (7), and accordingly, change the integrals to summation in the following manner:

$$E_\theta(\theta,\varphi) = \frac{-j\omega\mu_o a e^{-jk_o r}}{4\pi r} \sum_{k=1}^{K} [T_k(\varphi'_k)][Z_{jk}]^{-1}[V_j][\cos\theta\sin(\varphi-\varphi'_k) - \sin\theta\tan\alpha]e^{jk_o a\zeta\sin\theta}\Delta\varphi'_k, \tag{9a}$$

$$E_\varphi\,(\theta,\varphi) = \frac{-j\omega\mu_o a e^{-jk_o r}}{4\pi r} \sum_{k=1}^{K} [T_k(\varphi'_k)]\,[Z_{jk}]^{-1}[V_j]\,[\cos(\varphi-\varphi'_k)]e^{jk_o a\xi\sin\theta}\Delta\varphi'_k \tag{9b}$$

$$\zeta = \cos(\varphi-\varphi'_k) + (\tan\alpha\cot\theta)\varphi'_k. \tag{9c}$$

Of main interest in this presentation is the radiated electric fields of the chireix coil antenna in the azimuthal plane where $\theta = \pi/2$ because of the remarkable radiation characteristics of centre-fed microstrip helix in that plane [5]. Consequently, upon the substitution of $\theta = \pi/2$ in Equations (9a)–(9c) we readily obtained the following simplified expressions:

$$E_\theta\,(\pi/2,\varphi) \;=\; \frac{-j\omega\mu_o a e^{-jk_o r}}{4\pi r} \sum_{k=1}^{K} [T_k(\varphi'_k)]\,[Z_{jk}]^{-1}[V_j]\,[-\tan\alpha]e^{jk_o a\zeta}\Delta\varphi'_k, \tag{10a}$$

$$E_\varphi\,(\pi/2,\varphi) \;=\; \frac{-j\omega\mu_o a e^{-jk_o r}}{4\pi r} \sum_{k=1}^{K} [T_k(\varphi'_k)]\,[Z_{jk}]^{-1}[V_j]\,[\cos(\varphi-\varphi'_k)]e^{jk_o a\xi}\Delta\varphi'_k, \tag{10b}$$

$$\zeta \;=\; \cos(\varphi-\varphi'_k). \tag{10c}$$

The computational results obtained based on the above equations will now be discussed.

4. COMPUTATIONAL RESULTS

Before discussing the computational results generated for the chireix coil antenna, a comparison is made between the current distribution computed from Equation (7) at operating frequency of 500 MHz with the published theoretical and experimental results of [3] who provided a Fourier series solution of the current along a centre-fed thin-wire helix. The results of the comparative exercise for a 6-turn centre-fed helix are displayed in Figures 2(a) and (b), which clearly reveal

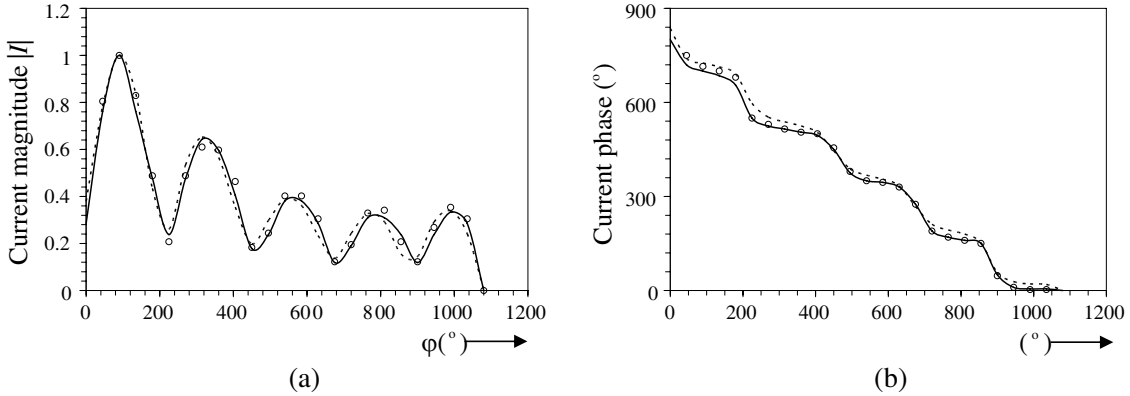

Figure 2: Comparison of current magnitude and phase of a centre-fed helical antenna at 500 MHz: – – – –: MoM; ———: Chen's theory and ∘ ∘ ∘∘: Experimental results at 500 MHz of Figure 6(a) [3].

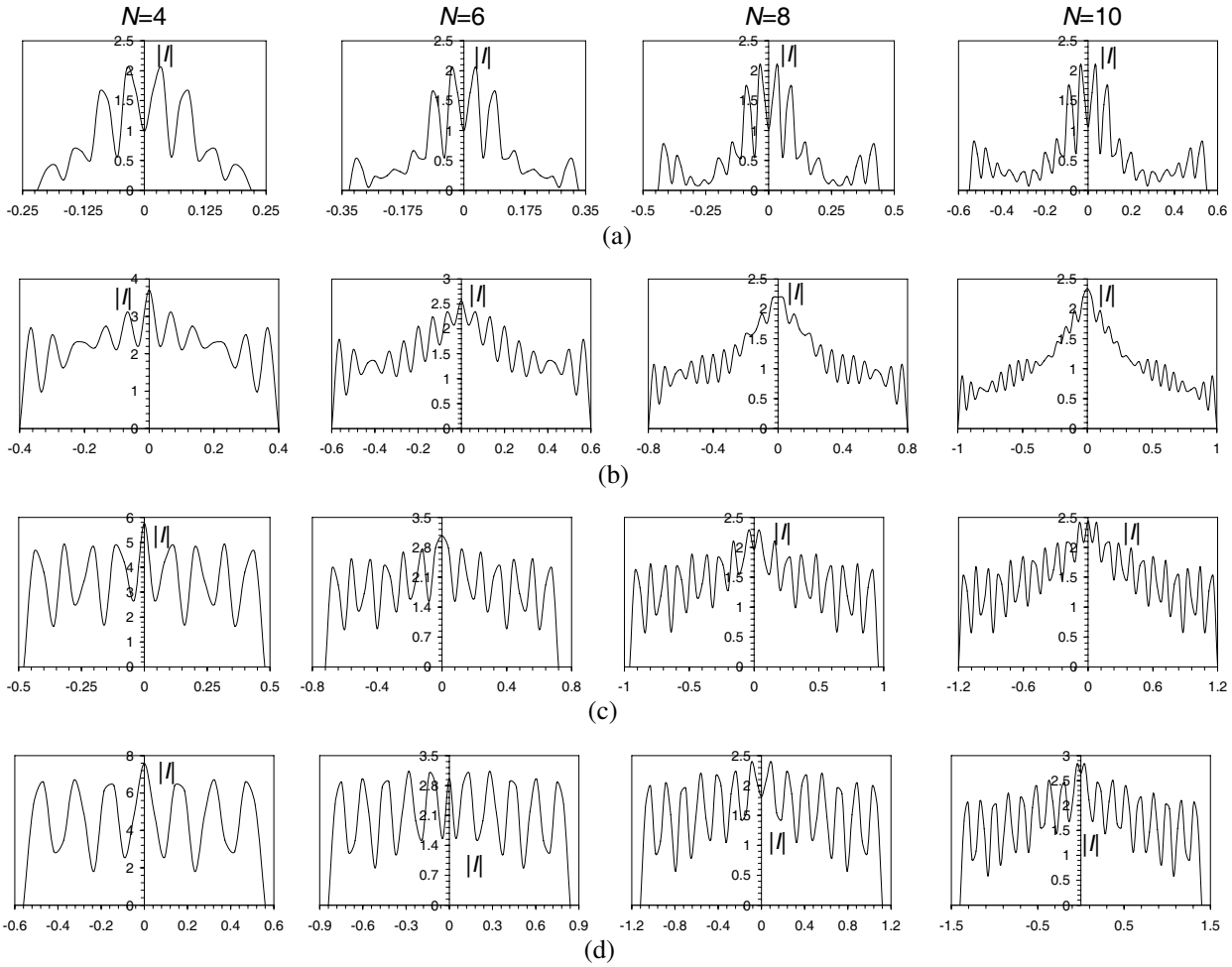

Figure 3: Current distributions along the arm length of Chireix coil antenna: $0.1 \leq S_\lambda \leq 1.8$. The horizontal axis represents the coil arm length. (a) $S_\lambda = 0.10$, (b) $S_\lambda = 1.0$, (c) $S_\lambda = 1.4$, (d) $S_\lambda = 1.8$.

good agreement between our MoM results and the Chen's results, and invariably lends credence to the MoM solution of the centre-fed helical antenna problem addressed in this paper.

The Chiriex coil geometry is mathematically defined by $C_\lambda = \sqrt{1+2S_\lambda}$ [2] where (C_λ, S_λ) symbolize helix circumference and turn-spacing expressed in wavelengths at the operating frequency, respectively. Consequently, the length of one turn of the helix is given by $L_\lambda = \sqrt{(1+2S_\lambda)^2 + S_\lambda^2} = 1+S_\lambda$ based on Figure 1(b). For numerical computations, the following values of relevant parameters

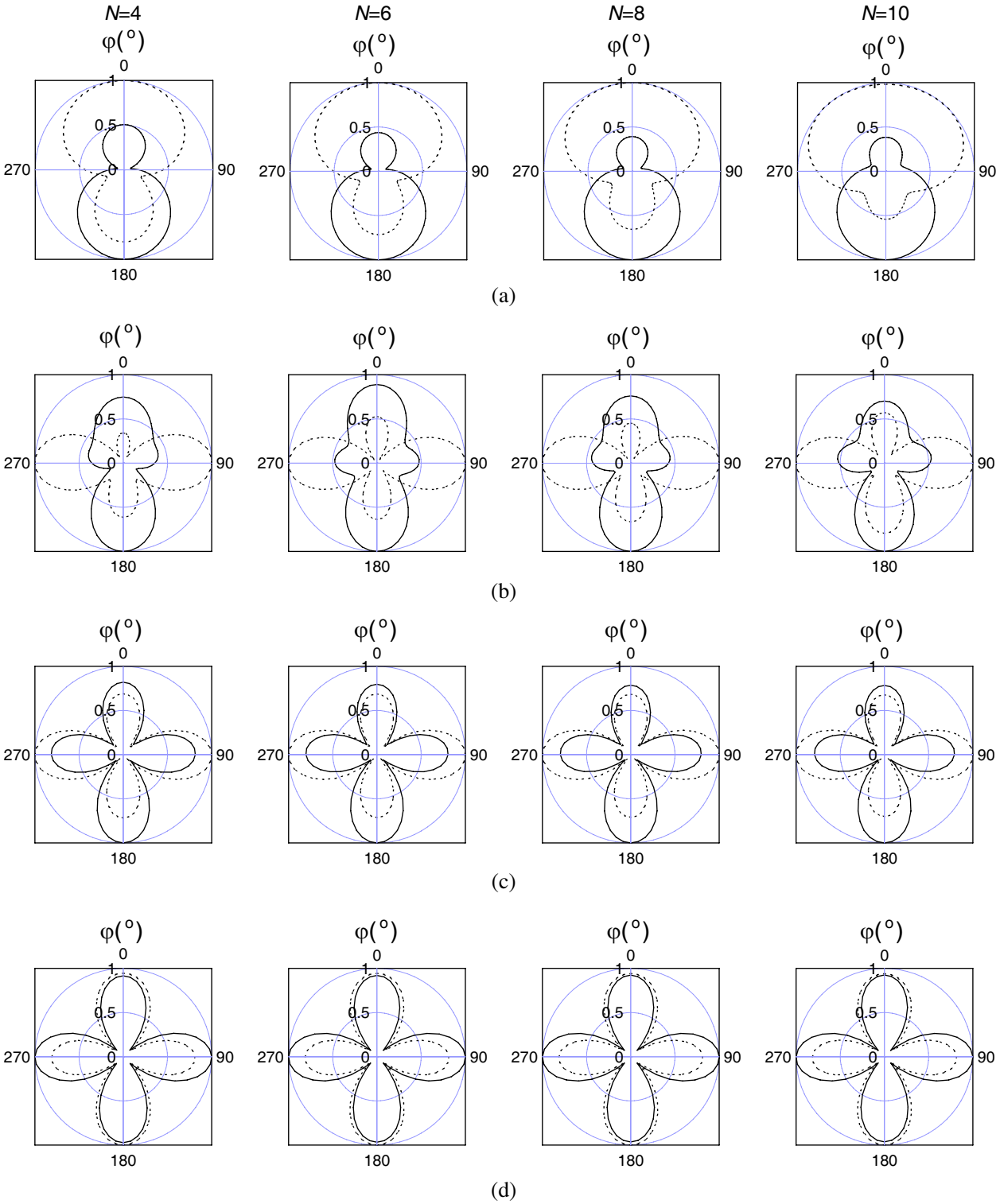

Figure 4: Electric field patterns on the azimuthal plane: ———: E_θ; - - - - - - - -: E_φ. (a) $S_\lambda = 0.1$, (b) $S_\lambda = 1.0$, (c) $S_\lambda = 1.4$, (d) $S_\lambda = 1.8$.

are utilized: $0.1 \leq S_\lambda \leq 1.8$, $1.095 \leq C_\lambda \leq 2.145$, $5.2^\circ \leq \alpha \leq 40^\circ$, $N = 4$, 6, 8, and 10, operating frequency = 3 GHz, wire radius (r_w) = 0.3 mm and the excitation voltage = 1.0 V.

4.1. Current Distributions

A cursory examination of Figure 3 clearly shows that the current profiles along the helical arm length are symmetrical about the feed-point which corresponds to the geometrical centre of the chiriex coil. It is also noticed that the maximum value of the magnitude of current distribution along the arm length is, to a large extent, independent of number of coil turns. Except for the scenario $S_\lambda = 1.0$ and $C_\lambda = \sqrt{3}$ that the current peaks occur at the feed-point regardless of the number of chireix coil turns, the other scenarios reported $S_\lambda = 0.1$, 1.4 and 1.8 are characterized by current peaks at or off the feed-point. In addition, for S_λ less than 1.0, the maximum value of current which is about 2.1 mA remains fairly unchanged irrespective of the number of coil turns. It is further observed that only the 4-turn coil enjoys steady increase in the current maximum as S_λ increases, other coil antennas (6-, 8- and 10-turn helices) have relatively constant maximum current of about 2.5 mA, perhaps this observation may be attributed to substantial reflections from the open ends due to the shortness of the 4-turn coil. And characteristic of all the current distributions is the several undulations along the helical arm regardless of the number of coil turns, a consequence of reflections from the two open ends of the antenna. Finally, it is worth remarking that for helix of several turns mounted on a large ground plane, its current is typified by a travelling wave that decays exponentially towards the open end [1]. Next, the corresponding electric field patterns in the azimuthal plane generated by the current distributions of Figure 3 are given consideration.

4.2. Electric Fields

Although only the E_θ and E_φ patterns for $S_\lambda = 0.1$ are displayed in Figure 4(a), it is noted that for $S_\lambda < 1.0$, the radiation field (E_θ, E_φ) patterns on the azimuthal plane ($\theta = \pi/2$) are characterized by two diametrically directed major lobes along $\varphi = 0^\circ$ and 180° irrespective of the number of coil turns. However, when S_λ equals 1.0, the degeneration of the aforementioned two majors into four major lobes begins for the 4-, 6-, 8-, and 10-turn Chireix coils investigated here. Remarkably at S_λ greater than 1.4, the four lobes have been fully developed and distinct with relative maxima along $\varphi = 0^\circ$, 90°, 180° and 270° axes. In general, these radiation field pattern features seem to be independent of the number of Chiriex coil turns. Thus, the Chiriex coil antenna may enjoy practical applications where multilobed radiation patterns are desirable.

5. CONCLUDING REMARKS

Presented here is the method of moment solution of the electric field integral equation (EFIE) governing the Chiriex coil antenna problem. In the main, attention was focused on the current distributions and associated azimuthal plane radiation characteristics of the antenna. It is found that the maximum value of current distributed along the antenna axis is somewhat independent of the number of coil turns, and when turn spacing is 1.8 wavelengths, the E_θ and E_φ patterns are characterized by four distinct lobes with relative maxima along $\varphi = 0^\circ$, 90°, 180° and 270° axes, which suggest possible deployment of the coil antenna for multi-lobed radiation patterns applications.

REFERENCES

1. Nakano, H. and J. Yamauchi, "Radiation characteristics of helix antenna with parasitic elements," *Electronics Letters*, Vol. 16, No. 18, 687–688, 1980.
2. Kraus, J. D., *Antennas*, 2nd Edition, 265–339, McGraw-Hill, Inc., USA, 1988.
3. Chen, C. L., "Theory of the balanced helical wire antenna," *Radio Science*, Vol. 2, No. 2, 167–190, 1967.
4. Roy, M. N., "Investigations on normal mode helices," *Int. J. Electronics*, Vol. 26, No. 6, 573–578, 1969.
5. Martin, R. A. and D. H. Werner, "A reciprocity approach for calculating the far-field radiation patterns of a centre-fed helical microstrip antenna mounted on a dielectric-coated circular cylinder," *IEEE Trans. Ant. & Prog.*, Vol. 49, No. 12, 1754–1762, 2001.
6. Harrington, R. F., *Field Computation by Moment Methods*, 125, The Macmillian Book Company, New York, 1968.